

# Silicon-chip-based mid-infrared dual-comb spectroscopy

Mengjie Yu,<sup>1,2</sup> Yoshitomo Okawachi,<sup>1</sup> Austin G. Griffith,<sup>3</sup>  
Nathalie Picqué,<sup>4,5,6</sup> Michal Lipson,<sup>7</sup> and Alexander L. Gaeta<sup>1,\*</sup>

<sup>1</sup>*Department of Applied Physics and Applied Mathematics, Columbia University, New York, NY 10027*

<sup>2</sup>*School of Electrical and Computer Engineering, Cornell University, Ithaca, NY 14853*

<sup>3</sup>*School of Applied and Engineering Physics, Cornell University, Ithaca, NY 14853*

<sup>4</sup>*Max-Planck-Institut für Quantenoptik, Hans-Kopfermann-Straße 1, 85748 Garching, Germany*

<sup>5</sup>*Ludwig-Maximilians-Universität München, Fakultät für Physik, Schellingstr. 4/III, 80799 München, Germany*

<sup>6</sup>*Institut des Sciences Moléculaires d'Orsay (ISMO), CNRS,*

*Univ. Paris-Sud, Université Paris-Saclay, F-91195 Orsay, France*

<sup>7</sup>*Department of Electrical Engineering, Columbia University, New York, NY 10027*

compiled: October 5, 2016

On-chip spectroscopy that could realize real-time fingerprinting with label-free and high-throughput detection of trace molecules is one of the "holy grails" of sensing. Such miniaturized spectrometers would greatly enable applications in chemistry, bio-medicine, material science or space instrumentation, such as hyperspectral microscopy of live cells or pharmaceutical quality control. Dual-comb spectroscopy (DCS) [1–19], a recent technique of Fourier transform spectroscopy without moving parts, is particularly promising since it measures high-precision spectra in the gas phase using only a single detector. Here, we present a microresonator-based platform designed for mid-infrared (mid-IR) DCS. A single continuous-wave (CW) low-power pump source generates two mutually coherent mode-locked frequency combs spanning from 2.6  $\mu\text{m}$  to 4.1  $\mu\text{m}$  in two silicon micro-resonators. Thermal control and free-carrier injection control modelocking of each comb and tune the dual-comb parameters. The large line spacing of the combs (127 GHz) and its precise tuning over tens of MHz, unique features of chip-scale comb generators, are exploited for a proof-of-principle experiment of vibrational absorption DCS in the liquid phase, with spectra of acetone spanning from 2870 nm to 3170 nm at 127-GHz ( $4.2\text{-cm}^{-1}$ ) resolution. We take a significant step towards a broadband, mid-IR spectroscopy instrument on a chip [20]. With further system development, our concept holds promise for real-time and time-resolved spectral acquisition on the nanosecond time scale.

Microresonator-based frequency comb generators represent an attractive emerging technology of compact and broadband sources emitting equidistant phase-coherent lines with a large line spacing using a single CW pump

laser [18, 21–29]. Their development in the mid-IR region is motivated by new approaches to absorption spectroscopy, one of the major techniques of non-intrusive analysis of matter. In particular, they would provide new capability for dual-comb spectroscopy, which measures the time-domain interference between two combs of slightly different line spacing. The potential of DCS is clear for gas-phase studies in the near-infrared spectral region where DCS shows higher measurement speed, resolution and accuracy than state-of-the-art Michelson-based Fourier transform spectrometers. As a result of extensive laser developments, such capabilities are currently being transferred in the mid-IR spectral region [2, 4, 7, 8, 10–12, 14, 16, 17], where most molecules have strong and characteristic fundamental absorption features. Such efforts however do not address optical systems suited for vibrational DCS in the liquid and solid-state phase, which would strongly take advantage of combs emitting over at least one octave with a line spacing of the order of the desired spectral resolution, i.e. higher than 100 GHz.

In this work, we present a CMOS-compatible silicon-based, chip-scale mid-IR dual-comb spectrometer that meets these requirements. The experimental setup is shown in Fig. 1. We use two silicon microresonators that have 100- $\mu\text{m}$  radii and are dispersion engineered to have anomalous group-velocity dispersion beyond 3  $\mu\text{m}$  for the fundamental TE mode, similar to Griffith, *et al.* [27]. A CW optical parametric oscillator (100-kHz linewidth) emitting at 3  $\mu\text{m}$  simultaneously pumps two microresonator-based frequency comb generators with slightly different line spacings. The two generated combs are combined at a beamsplitter and sent to a photodetector (bandwidth of 250 MHz) connected to an RF spectrum analyzer. Integrated PIN diodes are operated at a reverse-bias voltage of -15 V to sweep out

\* Corresponding author: alg2207@columbia.edu

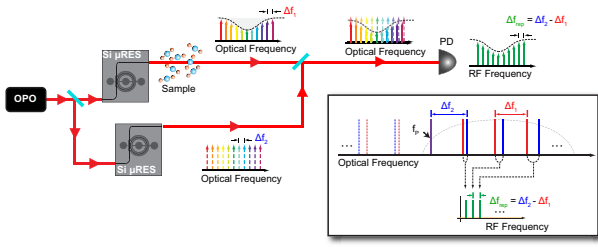


Fig. 1. Experimental setup for our dual-comb source. A continuous-wave optical parametric oscillator pumps two separate silicon microresonators, which generate two mode-locked combs. The output is combined and sent to a photodiode for RF characterization. Inset: Schematic for single-pump operation and mapping from optical to RF domain.  $\Delta f_1$  and  $\Delta f_2$  are the repetition frequencies of two optical frequency combs.  $\Delta f_{\text{rep}} = \Delta f_2 - \Delta f_1$  is the difference in repetition frequencies.

the free carriers (FC) generated from three-photon absorption (3PA) [25]. We generate a modelocked mid-IR frequency comb in both microresonators simultaneously by tuning the pump laser into the cavity resonances. A thermoelectric cooler (TEC) is used to control the temperature of each silicon device independently in order to compensate the initial frequency difference between the two pump resonances, and for coarse tuning of the difference in repetition frequencies between the two combs  $\Delta f_{\text{rep}}$  to lie within our detector bandwidth. Future implementations could allow for fully integrated microheaters<sup>29</sup>, which would achieve even more precise control of the line spacing of each of the microresonators while drawing little power. The mutual coherence between the two combs is established by sharing the same pump laser and from the inherent modelocking mechanism of microresonator-based combs. The RF beatnotes of the dual-comb output appear at frequencies  $f_N = N \cdot \Delta f_{\text{rep}}$ , where  $N$  is an integer. Figure 1 (inset) shows the mapping of the optical spectrum to the RF dual-comb spectrum where the shorter and longer wavelength sides of the pump are mapped to the same RF domain, which means appropriate long-pass/short-pass filters are needed to access either side of the optical spectrum relative to the pump frequency. Shifting the pump frequency of one of the microresonators, e.g., with an acoustic-optic modulator, would avoid such aliasing, as already demonstrated with electro-optic-modulator-based dual-comb spectroscopy [9, 13, 15, 16].

Figure 2a shows the generated spectrum of one of the combs measured by a Michelson-based Fourier transform infrared spectrometer (M-FT). The spectrum consists of 305 comb lines with a spacing  $f_{\text{rep}} = 127$  GHz and spans  $2.6 - 4.1 \mu\text{m}$ , which is the region of the fundamental CH, NH and OH stretching modes in molecules. The pump powers for each microresonator are 80 and 50 mW, and the pump-to-comb conversion efficiencies are each  $>30\%$ . Since the cavity linewidth ( $10^5$  Q-factor) is broader than the detector bandwidth, the sharp comb

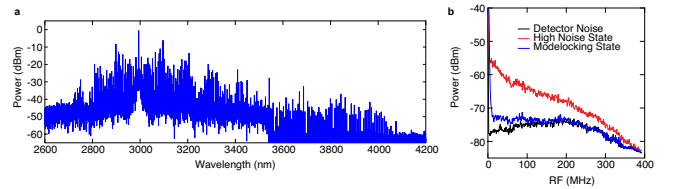


Fig. 2. (a) A spectrum of one of the generated combs measured using a Michelson-based Fourier transform infrared spectrometer (M-FT). The spectral range is from  $2.6 \mu\text{m}$  to  $4.1 \mu\text{m}$ . (b) RF-noise characterization of the generated comb. The plot shows the reduction in RF amplitude noise corresponding to modelocking.

linewidth when in the modelocked state is crucial for resolving the RF beatnotes of the two combs. The transition to the modelocked state is determined by the observation of a step in the optical transmission [24], an abrupt increase in the 3PA-induced FC current [28], and the transition to a low RF noise state as shown in Fig. 2b [22].

While the M-FT spectra of the two individual and combined modelocked frequency combs are shown in Fig. 3a, the RF dual-comb spectrum is plotted in Fig. 3b where the intensity profile agrees well with the product of the amplitudes of the electric fields of two optical frequency combs within the detection range. The achieved difference between the line spacings  $\Delta f_{\text{rep}}$  is 12.8 MHz, corresponding to a frequency compression factor from the optical to RF domain of  $f_{\text{rep}}/\Delta f_{\text{rep}}$  ( $\sim 10,000$ ). The minimum time required to resolve the RF comb lines is  $1/\Delta f_{\text{rep}}$  ( $\sim 78$  ns), indicating the potential for a rapid single-shot measurement. The measured linewidth of the 25th RF comb line [Fig. 3b inset] is  $< 100$  kHz at a RF resolution bandwidth of 40 kHz, which corresponds to a mutual coherence time between the two combs of  $>10 \mu\text{s}$ . The frequency jittering of the optical frequency combs is dominated by the pump laser [29]. Therefore, the coherence between the two generated combs is drastically improved because the effect of the pump noise is expected to be significantly minimized by sharing the same pump with the two microresonators.

While the spectral window of  $2.6 - 4.1 \mu\text{m}$  ( $73 - 115$  THz) can be mapped into an RF window of 2.5 GHz with  $\Delta f_{\text{rep}} = 12.8$  MHz, our measurement spectral range is currently  $3 - 3.12 \mu\text{m}$ , which is largely limited by our detector bandwidth of 250 MHz. Our detection range can be extended to cover the entire spectral window by using a faster detector or by controlling the repetition rate of the two combs to achieve a smaller  $\Delta f_{\text{rep}}$  (e.g., 1 MHz). Coarse tuning of the  $\Delta f_{\text{rep}}$  can be achieved by thermally tuning the resonances of one microresonator by one or more FSRs. In our case, we found that the  $\Delta f_{\text{rep}}$  is changed by  $\sim 126$  MHz by moving to the next resonance in one of the microresonators, which is about  $1/1000$  of the FSR. Additionally, we achieve fine tuning of  $\Delta f_{\text{rep}}$ . Figure 4 shows the repetition rate tuning of our dual-comb system. We observe that  $\Delta f_{\text{rep}}$  can

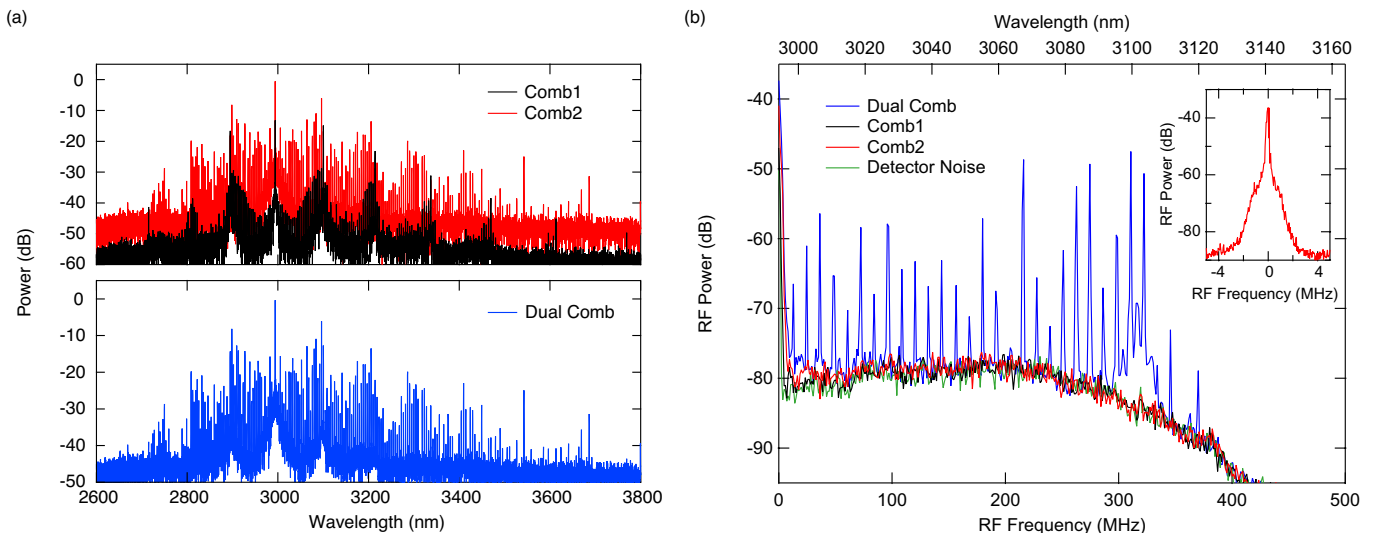


Fig. 3. (a) Top: M-FT spectra for each modelocked comb. Bottom: Combined M-FT spectrum. (b) RF spectrum from the dual-comb interferometer. Plot shows RF spectra for dual-comb (blue), each separate modelocked comb (black and red), and detector noise background (green). Inset: Characterization of the 25th RF beatnote in (b).

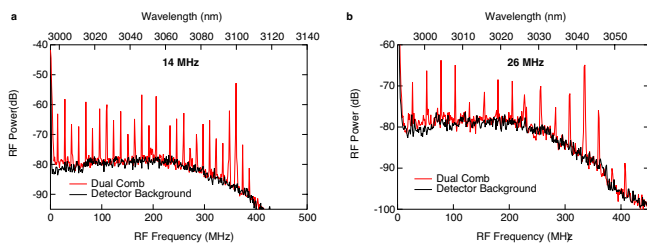


Fig. 4. The frequency spacing of the dual-comb source is dictated by the spacing of each of the modelocked combs. The plot shows a 14 MHz spacing (left) and a 26 MHz spacing. The spacing is tuned by adjusting the TECs to change the resonance position of the microresonators.

be finely tuned by  $>10$  MHz by simply changing the pump-cavity detuning while maintaining modelocking in both microresonators. Moreover,  $\Delta f_{\text{rep}}$  is dependent on both the FC dispersion effect and on the thermo-optic effect. By individually controlling the reverse-bias-voltage applied on the PIN junctions, the line spacings of the microresonators can be finely controlled independently such that smaller  $\Delta f_{\text{rep}}$  ( $\sim 1$  MHz) can be achieved in the near future. This tuning technique of the RF line spacing ( $\Delta f_{\text{rep}}$ ) provides flexibility in achieving an optimal refresh rate of the measurement over a desirable spectral range and in further compressing the needed RF window.

Finally, we illustrate the potential of our dual-comb spectrometer for broadband vibrational spectroscopy of liquid samples with a proof-of-principle absorption measurement. As shown in Fig. 1, we insert a 1-mm thick cuvette filled with neat acetone in one arm of the dual-comb interferometer. Such configuration also allows for measuring the dispersion spectra for broad spectral fea-

tures. Here, we utilize two different bandpass filters to access each side of the optical spectrum with respect to the pump wavelength. The absorption spectrum in the RF domain for both sides of the pump are measured using a photodetector of 1-GHz bandwidth, as shown in Fig. 5a corresponding to a spectral window of 2870 – 3170 nm. The measured spectrum with and without the acetone cuvette is shown in blue and red, respectively. Here the spacing of the RF comb lines is 33.7 MHz. The dual-comb transmittance spectrum shown in Fig. 5b is obtained by taking the ratio between the spectrum with acetone and the spectrum without acetone shown in Fig. 5a. A signal-to-noise ratio of 76,000 is achieved with a measurement time of 36 ms at a spectral resolution of 127-GHz ( $4.2\text{-cm}^{-1}$ ) resolution. We compared this spectrum to the transmittance spectrum we measured using a commercial mid-IR comb source (Menlo Systems) with a spectral window spanning 2.8 – 3.4  $\mu\text{m}$  with a 250-MHz line spacing and a grating-based optical spectrum analyzer. The two spectra show excellent agreement. With improvement to the acquisition system by time-domain sampling with a fast oscilloscope, higher acquisition rates and higher signal-to-noise ratios can be obtained in the near future.

In summary, we present a highly compact mid-IR dual-comb spectrometer using silicon-microresonator-based frequency combs pumped with a single pump source covering a broad optical spectrum from 2870 nm to 3170 nm, and as a proof-of-principle, we demonstrated broadband absorption measurement of acetone. With constant progress to instrumentation in the mid-IR and future developments to our CMOS-compatible platform, such as the implementation of quantum cascade continuous-wave lasers as pump sources, we envision a spectroscopy laboratory on a chip able of real-time

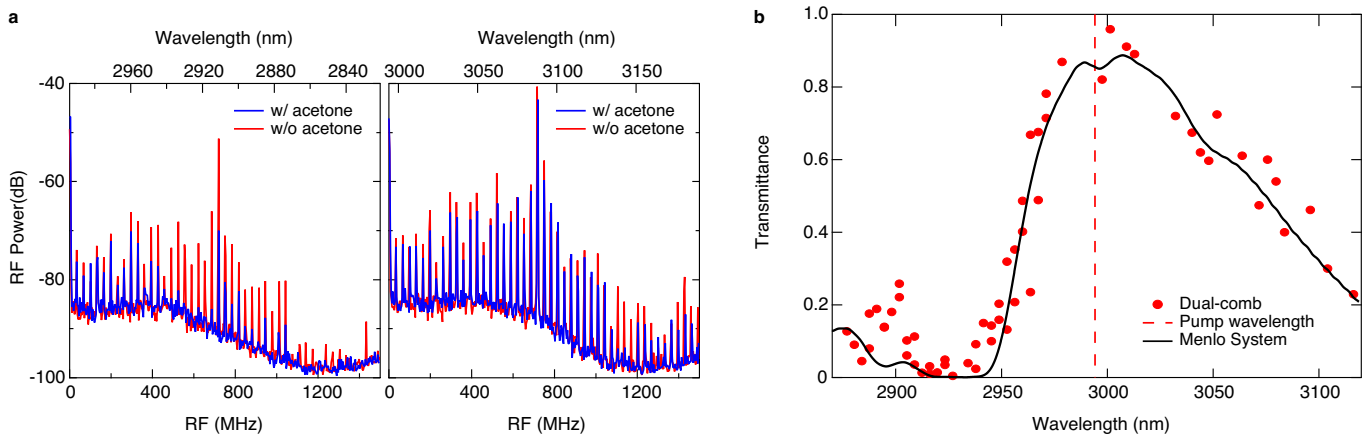


Fig. 5. (a) Dual-comb measurement using an RF spectrum analyzer. Two different bandpass filters are used to access the two sides of the dual-comb spectrum that are symmetric with respect to the pump. (b) Experimental characterization of the dual-comb absorption spectrum, which is calculated by taking the ratio between the spectrum with acetone and the spectrum without acetone. Each red dot is obtained at the wavelength position which matches the RF comb lines in (a).

vibrational sensing on the nanosecond time scale with a high signal-to-noise ratio, that operates over a broad bandwidth with access to other ranges of the molecular fingerprint region.

We thank Jun Ye from JILA, University of Colorado for useful discussions. We acknowledge support from Defense Advanced Research Projects Agency (W31P4Q-15-1-0015), the Air-Force Office of Scientific Research (FA9550-15-1-0303), and National Science Foundation (ECS-0335765, ECCS-1306035). This work was performed in part at the Cornell Nano-Scale Facility, a member of the National Nanotechnology Infrastructure Network, which is supported by the National Science Foundation (NSF) (grant ECS-0335765).

## References

- [1] Coddington, I., Newbury, N. & Swann, W. Dual-comb spectroscopy. *Optica* **3**, 414-426 (2016).
- [2] Bernhardt, B. *et al.* Mid-infrared dual-comb spectroscopy with 2.4  $\mu\text{m}$   $\text{Cr}^{2+}:\text{ZnSe}$  femtosecond lasers. *Appl. Phys. B* **100**, 3-8 (2010).
- [3] Bernhardt, B. *et al.* Cavity-enhanced dual-comb spectroscopy. *Nat. Photon.* **4**, 55-57 (2010).
- [4] Baumann, E. *et al.* Spectroscopy of the methane  $\nu_3$  band with an accurate midinfrared coherent dual-comb spectrometer. *Phys. Rev. A* **84**, 062513 (2011).
- [5] Ideguchi, T., Bernhardt, B., Guelachvili, G., Hnsch, T. W. & Picqué, N. Raman-induced Kerr-effect dual-comb spectroscopy. *Opt. Lett.* **37**, 4498-4500 (2012).
- [6] Ideguchi, T. *et al.* Coherent Raman spectro-imaging with laser frequency combs. *Nature* **502**, 355-358 (2013).
- [7] Zhang, Z., Gardiner, T. & Reid, D. T. Mid-infrared dual-comb spectroscopy with an optical parametric oscillator. *Opt. Lett.* **38**, 3148-3150 (2013).
- [8] Villares, G., Hugé, Blaser, S. & Faist, J. Dual-comb spectroscopy based on quantum-cascade-laser frequency combs. *Nat. Commun.* **5**, 5192 (2014).
- [9] Long, D. A. *et al.* Multiheterodyne spectroscopy with optical frequency combs generated from a continuous-wave laser. *Opt. Lett.* **39**, 2688-2690 (2014).
- [10] Wang, Y., Soskind, M. G., Wang, W. & Wysocki, G. High-resolution multi-heterodyne spectroscopy based on Fabry-Perot quantum cascade lasers. *Appl. Phys. Lett.* **104**, 031114 (2014).
- [11] Jin, Y., Cristescu, S. M., Harren, F. J. M. & Mandon, J. Femtosecond optical parametric oscillators toward real-time dual-comb spectroscopy. *Appl. Phys. B* **119**, 65-74 (2015).
- [12] Cruz, F. C. *et al.* Mid-infrared optical frequency combs based on difference frequency generation for molecular spectroscopy. *Opt. Express* **23**, 26814-26824 (2015).
- [13] Martin-Mateos, P., Jerez, B. & Acedo, P. Dual electro-optical frequency combs for multiheterodyne molecular dispersion spectroscopy. *Opt. Express* **23**, 21149-21158 (2015).
- [14] Zhu, F. *et al.* Mid-infrared dual frequency comb spectroscopy based on fiber lasers for the detection of methane in ambient air. *Laser Phys. Lett.* **12**, 095701 (2015).
- [15] Durn, V., Tainta, S. & Torres-Company, V. Ultrafast electrooptic dual-comb interferometry. *Opt. Express* **23**, 30557-30569 (2015).
- [16] Yan, M. *et al.* Mid-infrared dual-comb spectroscopy with electro-optic modulators. arXiv:1608.08013.
- [17] Smolski, V. O., Yang, H., Xu, J. & Vodopyanov, K. L. Massively parallel dual-comb molecular detection with subharmonic optical parametric oscillators. arXiv:1608.07318.
- [18] Suh, M.-G., Yang, Q.-F., Yang, K. Y., Yi, X. & Vahala, K. J. Microresonator soliton dual-comb spectroscopy. arXiv:1607.08222.
- [19] Schliesser, A., Picqué, N. & Hänsch, T. W. Mid-infrared frequency comb. *Nat. Photon.* **6**, 440-449 (2012).
- [20] Soref, R. Mid-infrared photonics in silicon and germanium. *Nat. Photon.* **4**, 495-497 (2010).
- [21] Kippenberg, T. J., Holzwarth, R. & Diddams, S. A. Microresonator-based optical frequency combs. *Science* **332**, 555-559 (2011).
- [22] Saha, K. *et al.* Modelocking and femtosecond pulse gen-

- eration in chip-based frequency combs, *Opt. Express* **21**, 1335-1343 (2013).
- [23] Wang, C. Y. *et al.* Mid-infrared optical frequency combs at 2.5  $\mu\text{m}$  based on crystalline microresonators. *Nat. Commun.* **4**, 1345 (2013).
- [24] Herr, T. *et al.* Temporal solitons in optical microresonators, *Nat. Photon.* **8**, 145-152 (2014).
- [25] Griffith, A. G. *et al.* Silicon-chip mid-infrared frequency comb generation. *Nat. Commun.* **6**, 6299 (2015).
- [26] Luke, K., Okawachi, Y., Lamont, M. R. E., Gaeta, A. L. & Lipson, M. Broadband mid-infrared frequency comb generation in a  $\text{Si}_3\text{N}_4$  microresonator. *Opt. Lett.* **40**, 4823-4826 (2015).
- [27] Griffith, A. G. *et al.* Coherent mid-infrared frequency combs in silicon-microresonators in the presence of Raman effects. *Opt. Express* **24**, 13044-13050 (2016).
- [28] Yu, M., Okawachi, Y., Griffith, A. G., Lipson, M. & Gaeta, A. L. Mode-locked mid-infrared frequency combs in a silicon microresonator. *Optica* **3**, 854-860 (2016).
- [29] Joshi, C. *et al.* Thermally controlled comb generation and soliton modelocking in microresonators. *Opt. Lett.* **41**, 2565 (2016).